Monitoring Acoustic Emission (AE) Energy of Abrasive Particle Impacts in a Slurry Impingement Flow Loop

Ghazi DROUBI *, Bob REUBEN **
*School of Engineering, Robert Gordon University, Aberdeen, UK
** School of Engineering and Physical Sciences, Heriot-Watt University, Edinburgh, UK

Abstract. The estimation of energy dissipated during multiple particle impact is a key aspect in evaluating the abrasive potential of particle-laden streams. A systematic investigation of particle impact energy using acoustic emission (AE) measurements was carried out to evaluate the influence of particle size, free stream velocity, and nominal particle concentration on the amount of energy dissipated in a carbon steel target using a slurry impingement flow loop test rig. Silica sand particles of mean particle size (225 to 650 μm) were used for impingement on the target with nominal concentration between 1 and 5% while the free stream velocity was changed between 4.2 and 14 ms^{-1}.

The measured AE energy was found to be proportional to the incident kinetic energy of the particles, although the high arrival rate involved in the slurry impingement flow loop poses challenges in resolving individual particle impact signatures in the AE record.The results have been reconciled with earlier work by the authors on sparse streams where there are few particle overlaps and good control over particle kinetic energies, by extending their model to account for different particle carrier-fluids and to situations where arrivals cannot necessarily be resolved.

Introduction

It is well-established [e.g. 1-3]that the rate of dissipation of the kinetic energy of impacting particles in a flow is related to the rate of material removal. Also, there is a general agreement that the AE energy associated with particle impingement is proportional to the incident kinetic energy $\frac{1}{2}mv^2$ [e.g. 4, 5]. Monitoring of particle impact using acoustic emission (AE) relies upon a fraction of the incident kinetic energy of each impacting particle dissipating as elastic waves, which propagate through the target material before being detected by a suitably placed AE sensor. Some of the investigators in this area have concentrated on monitoring the erosion variables [6], and others have concentrated on monitoring the amount of erosion [7]. The current authors [5, 8] have previously developed a model based on a probability distribution of particle impact energy, validated under controlled conditions of impingement.The purpose of this relatively uncontrolled impingement experiment was to assess what further adjustments need to be made in the processing to use AE as a semi-quantitative diagnostic indicator for particle impingement in real process flows.

Experimental method

The experimental set-up (Figure 1) used an AE system with a carbon steel target assembly identical to those used for earlier tests using air jet [8] and slurry impingement [5]. The flow loop consisted of a positive displacement pump (model C22BC10RMB, Mono pumpdriven by a 1.1 kW geared motor to give an output speed of 587 rpm), standard 25 mm PVC piping, a 50 litre conical tank and choke valves. The slurry was first mixed by recirculating it through a by-pass leg for around 20 minutes to ensure that all the solids were suspended in the flow before diverting the flow to the bend.

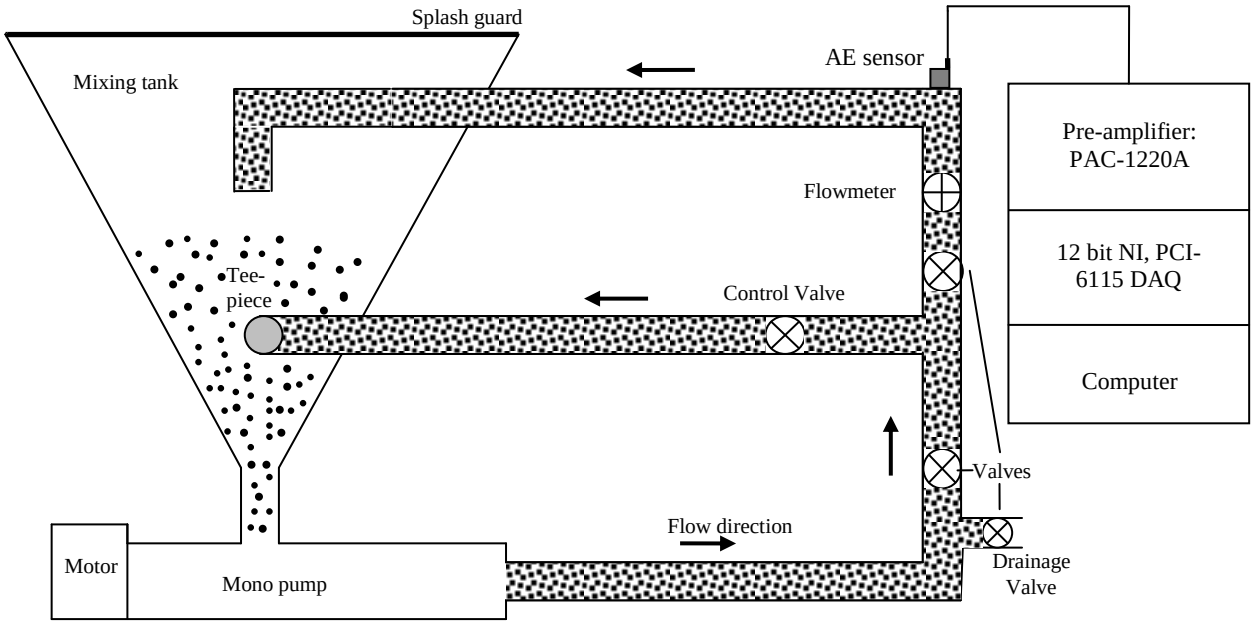

Figure 1: Sketch of the experimental flow loop with AE measurement system

The bend was made from 5 mm bore carbon steel inserted into the 23 mm bore PVC pipe, a sharp (90º) bend having been selected in order to localize the impingement area and minimize the impact angle range. The pipe wall opposite to the stream was milled flat in order to have a plane area to mount the AE sensor and the bend was machined to give an internal bore of 5 mm with a conical transition, giving 7 mm wall thickness at the site where the sensor was mounted. The length of the target section was 75 mm giving an overall impingement area similar to the other studies.The AE sensor was mounted using the magnetic clamp and coupled by means of vacuum grease to the opposite surface of the bend directly above the impingement area and the pre-amplified data were acquired at 2.5 MS/second for a record length of 1 second. Prior to testing, the sensitivity of the sensor was checked by performing a pencil lead break test at the bend to check the functioning of the AE detection system and to confirm the quality of sensor coupling.

Silica sand slurry was made from 10 litres of clean water and a predetermined mass of different particle size fractions in order to obtain the required concentration. Four different particle size ranges were used and, for each particle size range, an impingement run was carried out with a total of three levels of solid concentration (1, 2.5, and 5wt%) and four different flow velocities (4.2, 6.8, 10.2, and 12.7 ms^{-1}). The average particle launch rate was assessed by multiplying the volumetric flow rate by the average measured concentration and dividing by the average mass of a particle, giving values from around2.5×10^{4} to 2.5×10^{6} particles per second.

The AE energy measured was based on at least ten repeat records making a total of 120 AE records for each particle size range tested.Following each set of experiments, the rig was drained and cleaned.

The background noise AE energy associated with particle-free water impingementand the variability in AE energy associated with sensor removal and replacement between experiments was assessed in three testsbetween which the sensor was demounted and reinstalled, running clean water at each of the four flow speeds. **Figure 2** shows the recorded AE energy at each of thespeeds for each of the three experiments where each point represents the average of ten 1-second AE energy values along with its standard deviation. As can be seen, the variation in the energy recorded for each sensor installation (within group variation) is small, while the variation between installations is slightly larger.

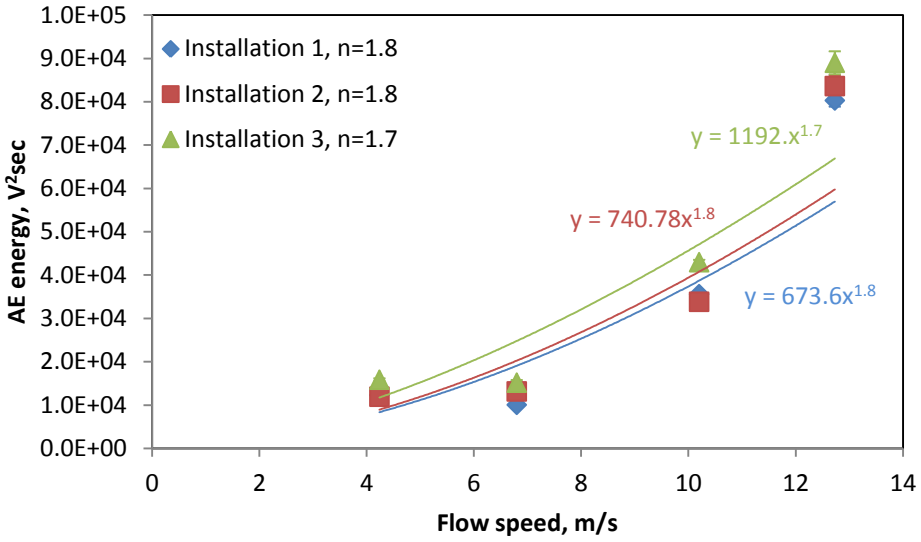

Figure 2: Recorded AE energy for pure water impingement in flow loop

Experimental results

For each experimental condition, the AE energy was calculated from the raw signal (measured as an amplified voltage, V) by integrating over the entire record:

$$E = \int_0^t V^2(t)dt$$

At least ten repeat 1-second records were analysed for each condition and the average value is used in the following general analysis to establish the effects of flow speed, particle size, and concentration, against the normal expectationthat energy will depend on the square of the impact speed, the cube of the particle diameter (i.e. the particle mass) and be linear with concentration expressed as mass per unit volume of water.

Figure3 shows one example of the effect of the flow speed (v) on the measured AE energy for the largest particle size range and all concentrations. As can be seen, the measured AE energy increases with both flow speed and concentration following approximately the second power of flow speed. **Table 2** summarises the results for all particle size ranges and all concentrations. As can be seen, the flow speed exponent is close to the expected value of 2 for all particle size ranges except the lowest size fraction where the signal:noise might be expected to be low. The variation of the best fit power index for

all experiments along with the respective correlation coefficients are also summarised in **Table 2** which shows the weighted average exponent to be 2.

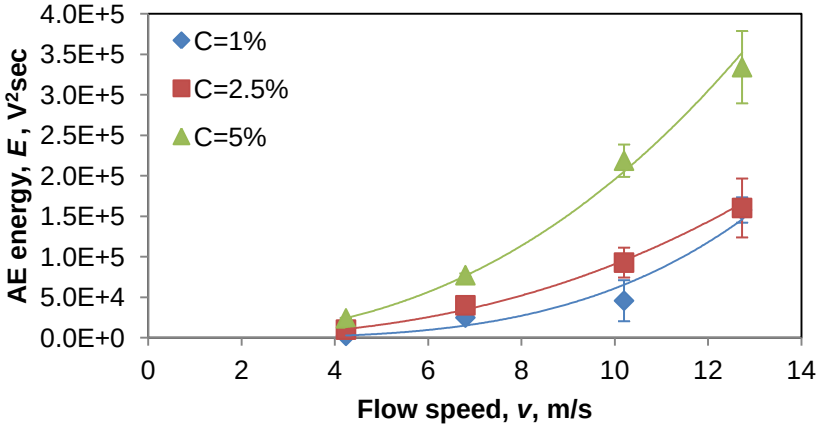

Figure 3: Effect of flow speed on the measured AE energy for the three concentrations for particle size range 600-710 µm

Table 2: Exponent of flow speed dependence of measured AE energy and correlation coefficient for all experiments (bold text data are shown in Figure 3)

Particle size range (µm)	Nominal concentration (kg/m^3)	Flow speed exponent (*n*)	Curve fitting R^2 value (%)
212-250	1	-	-
	2.5	0.45	36
	5	0.63	91
300-425	1	2.5	97
	2.5	1.9	98
	5	2	96
500-600	1	2	88
	2.5	1.8	94
	5	2.2	94
600-710	**1**	**3.6**	**95**
	2.5	**2.5**	**99**
	5	**2.4**	**99**

Table 3 lists the best fit power index for the effect of mean particle diameter on the measured AE energy for all measurements. Generally, the energy varies with approximately the third power of the mean particle diameter, except in the case of low speed where there is very little particle signal (above the water "noise") and where changes are difficult to discern at all. As for the flow speed exponent the diameter exponent tends towards the expected value of 3 at higher concentrations whereas, at the lower speeds and concentrations, the exponent tends towards 2 (in cases where a change can be discerned), leading to a weighted mean exponent of 2.6.

Finally, **Table 4** summarises the effect of nominal solid concentration on the measured AE energy for all particle size ranges. The resulting average values of the ten AE records at each condition show a general increase in AE energy with concentration for all particle sizes at all flow speeds, although there is a considerable scatter at higher flow speeds. The nominal concentration exponent tends towards the expected value of unity except in cases

of larger particle sizes and flow speeds where a drop out phenomenon might play a significant role. The weighted average exponent was 0.95.

Table 3: Exponent of particle size dependence of measured AE energy for all experiments

Nominal concentration (kg/m^3)	Flow speed (m/s)	Particle diameter exponent (φ)	Curve fitting R^2 value (%)
1	4.2	0.8	17
	6.8	3.3	97
	10.2	3.8	92
	12.7	4.8	91
2.5	4.2	1.5	79
	6.8	2	97
	10.2	3.2	88
	12.7	3.2	94
5	4.2	0.95	74
	6.8	1.8	81
	10.2	2.4	80
	12.7	2.75	85

Table 4: Exponent of particle concentration dependence of measured AE energy for all experiments

Particle size range (µm)	Flow speed (m/s)	Solid concentration exponent (β)	Curve fitting R^2 value (%)
212-250	4.2	0.76	80
	6.8	1.5	95
	10.2	1.6	98
	12.7	1.6	99
300-425	4.2	1.4	99
	6.8	1.1	99
	10.2	1.3	99
	12.7	0.9	82
500-600	4.2	0.25	84
	6.8	0.37	93
	10.2	0.46	99
	12.7	0.3	72
600-710	4.2	1.4	99
	6.8	0.7	97
	10.2	1	98
	12.7	0.45	69

Discussion

Given that the measured energy shows roughly the expected variation with speed, particle density and particle size, it remains to be seen whether the energy measured corresponds to what would be expected from a previously-developed log-normal distribution function[5] to

describe the probability distribution of particle arrival AE energy for air-propelled particles using the same target and sensor. The mean of the log-normal distribution function was found to be:

$$meanp.d.f = 1.7621\, mV^2 + 1 \times 10^{-5}$$

The expected AE energy in a population of impacts,$E_{calculated}$, can now be obtained using the average particle arrival rate (assumed to be the same as the launch rate) and the mean of the energy distribution function. The measured AE energy associated with the particles, $E_{measured}$, was estimated by subtracting the background water impingement energy $E_w$from the integral of the signal,

$$E_{measured} = E - E_w$$

whereE_w was obtained from the average of the correlation functions shown in Figure 2. The empirical model of Turenne and Fiset[9] was used to calculate the average particle speed for all the conditions studied.

Figures 4 and 5 show examples of the correlation between the calculated and the measured AE energy for each of the particle sizes using the average calculated impact speed. It is clear from these figures that the correlation slope approaches the expected value of unity with increasing particle size. This might be explained by the fact that smaller particle fractions (less inertia) are more vulnerable to influences of the fluid than bigger fractions (bigger inertia), which would change the impact angle and also the proportion of particles striking the surface, and this would also explain the lower measured values in **Figure 4**where uncontrolled behaviour of particles sweeping around the bend is more likely. **Figure 6** shows the average slope of the correlation between calculated AE energy and measured AE energy when taking all the data together. As can be seen, the slope is close to unity, although, the calculated (expected) AE energy is slightly overestimated. This might partly be explained by particle trajectories around the bend generally having an angle of incidence influenced by the bulk fluid flow, resulting in a greater proportion of particles having an angle of impact less than 90^o, and thus overestimating the calculated AE energy. Another possible reason might be that the hydraulic differences between the bend and the slurry impingement rig result in a smaller proportion of particles actually striking the target and contributing to AE energy due to a higher degree of particle interaction at or near the surface, resulting in particle collisions, reduced particle impact velocities and changed impact angles. Also, the effect of the slightly different design of the target at the bend might provide a leakage path for AE energy reducing the amount of measured AE energy. These factors have probably all contributed to the overestimate in the calculated AE energy and are those which would have to be taken into account in any real application of the technique as they are dependent on the design of the system being monitored.

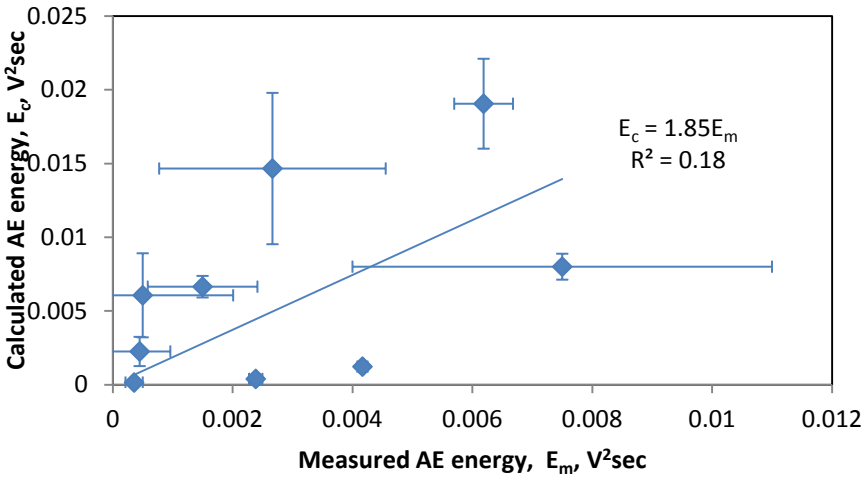

Figure 4: Calculated AE energy versus measured AE energy for particle size range 212-250 µm

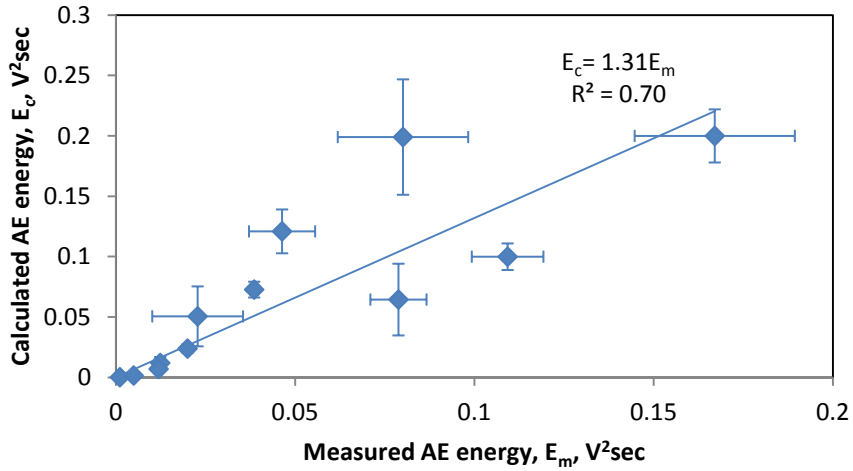

Figure 5: Calculated AE energy versus measured AE energy for particle size range600-710 µm

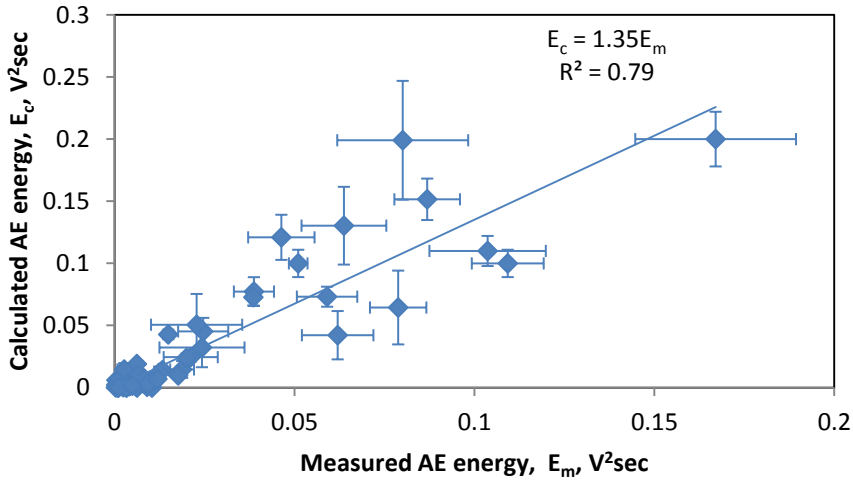

Figure 6: Calculated AE energy versus measured AE energy for all particle size ranges investigated

Conclusion

A series of slurry impingement tests were carried out to study the effect of particle size, flow speed, and particle concentration, on the AE energy dissipated in a carbon steel bend, with the following broad findings:

1. The measured AE energy was found overall to be proportional to the expected square of velocity, cube of particle size, and linear with concentration of the incident flow over a wide range of particle sizes (125-600 µm), flow speeds (4-12 ms^{-1}), and nominal concentrations (1-5 wt%), but, again, with weaker expression for smaller, slower particles.

2. The calculated AE energy (from the model) showed good agreement with the measured AE energy, but with the model overestimating the energy slightly, particularly for smaller particles. The discrepancies could be traced to details of the design of the hydraulics and the target, and these are factors which would need to be accounted for in any practical application.

3. In combining the fluid mechanics of particles suspended in liquid and the model, this model of AE energy can be used as a semi-quantitative diagnostic indicator for particle impingement in industrial equipment such as pipe bends.

References

1. Clark H M and Wong K K, *Impact angle, particle energy and mass loss in erosion by dilute slurries.* Wear, 1995, **186-187**(Part 2), pp. 454-464.
2. Head W J and Harr M E, *The development of a model to predict the erosion of materials by natural contaminants.* Wear, 1970, **15**(1), pp. 1-46.
3. Burstein G T and Sasaki K, *Effect of impact angle on the slurry erosion-corrosion of 304L stainless steel.* Wear, 2000, **240**(1-2), pp. 80-94.
4. Buttle D J and Scruby C B, *Characterization of particle impact by quantitative acoustic emission.* Wear, 1990, **137**(1), pp. 63-90.
5. Droubi M G, Reuben R L and G. White, *Statistical distribution models for monitoring acoustic emission (AE) energy of abrasive particle impacts on carbon steel.* Mechanical Systems and Signal Processing, 2012, **30**, pp. 356-372.
6. Hou R, Hunt A and Williams R A, Acoustic monitoring of pipeline flows: particulate slurries. Powder Technology, 1999, 106(1-2), pp. 30-36.
7. Ferrer F *et al.*, *On the potential of acoustic emission for the characterization and understanding of mechanical damaging during abrasion-corrosion processes.* Wear, 1999, **231**(1), pp. 108-115.
8. Droubi M G, Reuben R L and White G, *Acoustic Emission (AE) monitoring of abrasive particle impacts on carbon steel.* Proceedings IMechE, Part E, Journal of Process Mechanical Engineering, 2012,**226**(3), pp. 187-204.
9. Turenne S and Fiset M, *Modeling of abrasive particle trajectories during erosion by a slurry jet.* Wear, 1993, **162-64** (pt. B), pp. 679-687.